

Neuron

Loss and Gain of MeCP2 Cause Similar Hippocampal Circuit Dysfunction that Is Rescued by Deep Brain Stimulation in a Rett Syndrome Mouse Model

Highlights

- Shared CA1 circuit dysfunction in both MeCP2 loss- and gain-of-function models
- MeCP2 loss in excitatory and inhibitory neurons differently drives hypersynchrony
- Reduced excitatory synaptic response in oriens-layer interneurons upon loss/gain of MeCP2
- DBS rescues neural circuit dysfunction in hippocampal CA1 of Rett mice

Authors

Hui Lu, Ryan T. Ash, Lingjie He, ..., Benjamin R. Arenkiel, Stelios M. Smirnakis, Huda Y. Zoghbi

Correspondence

hzoghbi@bcm.edu

In Brief

MeCP2 loss and gain cause similar cell-type-dependent synaptic and circuit dysfunction in the hippocampus. Chronic forniceal deep brain stimulation that rescues hippocampus-dependent learning and memory in *Mecp2*^{+/-} (Rett) mice also rescues circuit dysfunction in these mice.



Loss and Gain of MeCP2 Cause Similar Hippocampal Circuit Dysfunction that Is Rescued by Deep Brain Stimulation in a Rett Syndrome Mouse Model

Hui Lu,^{1,4,9} Ryan T. Ash,^{2,3,9} Lingjie He,^{1,4,8} Sara E. Kee,² Wei Wang,^{1,4} Dinghui Yu,^{1,6} Shuang Hao,^{1,6} Xiangling Meng,^{1,2} Kerstin Ure,^{1,4} Aya Ito-Ishida,^{1,4} Bin Tang,^{1,6} Yaling Sun,^{1,8} Daoyun Ji,^{2,7} Jianrong Tang,^{1,6} Benjamin R. Arenkiel,^{1,2,4} Stelios M. Smirnakis,^{2,5,10} and Huda Y. Zoghbi^{1,2,4,5,6,8,*}

¹Jan and Dan Duncan Neurological Research Institute, Texas Children's Hospital, Houston, TX 77030, USA

²Department of Neuroscience

³Medical Scientist Training Program

⁴Department of Molecular and Human Genetics

⁵Department of Neurology

⁶Department of Pediatrics

⁷Department of Molecular and Cellular Biology

⁸Howard Hughes Medical Institute,

Baylor College of Medicine, Houston, TX 77030, USA

⁹Co-first author

¹⁰Present address: Department of Neurology, Brigham and Women's Hospital, Jamaica Plain VA Hospital, Harvard Medical School, Boston, MA 02115, USA

*Correspondence: hzoghbi@bcm.edu

<http://dx.doi.org/10.1016/j.neuron.2016.07.018>

SUMMARY

Loss- and gain-of-function mutations in methyl-CpG-binding protein 2 (*MECP2*) underlie two distinct neurological syndromes with strikingly similar features, but the synaptic and circuit-level changes mediating these shared features are undefined. Here we report three novel signs of neural circuit dysfunction in three mouse models of *MECP2* disorders (constitutive *Mecp2* null, mosaic *Mecp2*^{+/-}, and *MECP2* duplication): abnormally elevated synchrony in the firing activity of hippocampal CA1 pyramidal neurons, an impaired homeostatic response to perturbations of excitatory-inhibitory balance, and decreased excitatory synaptic response in inhibitory neurons. Conditional mutagenesis studies revealed that MeCP2 dysfunction in excitatory neurons mediated elevated synchrony at baseline, while MeCP2 dysfunction in inhibitory neurons increased susceptibility to hypersynchronization in response to perturbations. Chronic fornical deep brain stimulation (DBS), recently shown to rescue hippocampus-dependent learning and memory in *Mecp2*^{+/-} (Rett) mice, also rescued all three features of hippocampal circuit dysfunction in these mice.

INTRODUCTION

Deletion or duplication of specific genes causes neurodevelopmental disease, and, surprisingly, the loss- and gain-of-function

disorders for a given gene often have overlapping neurological symptoms. Rett syndrome and *MECP2* duplication syndrome are good examples: Rett syndrome is caused by loss-of-function mutations in the gene encoding methyl-CpG-binding protein 2 (MeCP2), whereas *MECP2* duplication syndrome is caused by duplication of the genomic region that spans *MECP2* in Xq28. Although the syndromes are distinct, and mouse models of these disorders show inverse patterns of gene expression (Chahrour et al., 2008), synapse strength and number (Chao et al., 2007), synaptic plasticity (Chahrour and Zoghbi, 2007; Collins et al., 2004), and dendritic arborization (Jiang et al., 2013), the Rett and *MECP2* duplication syndrome phenotypes overlap as the full-blown syndromes develop. Both produce autism features, seizures, motor impairments, stereotyped behaviors, and intellectual disability (Chahrour and Zoghbi, 2007; Ramocki et al., 2010). The mechanism accounting for overlapping phenotypes in two syndromes with opposite molecular defects (and transcriptional alterations) remains mysterious.

Learning disability is a common phenotype of both Rett syndrome and *MECP2* duplication syndrome (Chahrour and Zoghbi, 2007; Ramocki et al., 2010). During learning, the hippocampus receives stimuli relevant to the training experience from the cortex (Mehta, 2015). Optimal function of the hippocampal circuit depends on asynchronous, sparse firing activity (Huxter et al., 2003; Renart et al., 2010). A range of homeostatic mechanisms actively generates this asynchronous neural circuit state by mediating the balance between synaptic excitation and inhibition (Okun and Lampl, 2008). Impairment in these mechanisms leads to a loss of the asynchronous network state, resulting in populations of neurons firing in synchrony (Uhlhaas and Singer, 2006), even in the absence of stimulation at the baseline state. Excessive neuronal population synchrony disrupts complex

circuit dynamics, impairing normal information processing (Gonçalves et al., 2013; Luongo et al., 2016).

Given that *MECP2* deletion and duplication syndromes both result in learning disability, and the close relationship between learning and memory and hippocampal function, we hypothesized that the opposing molecular defects in these disorders lead to shared abnormalities in hippocampal circuit function and homeostasis. To explore this hypothesis, we used in vivo and ex vivo electrophysiology, two-photon calcium imaging, conditional mouse genetics, and forniceal deep brain stimulation (DBS).

RESULTS

Female mice lacking one *Mecp2* allele (Rett model, *Mecp2*^{+/-}) (Guy et al., 2001) or expressing an extra copy of the human *MECP2* allele (*MECP2* duplication syndrome model) (Collins et al., 2004) were crossed to transgenic animals that express the genetically encoded calcium indicator GCaMP3 in excitatory neurons (*thy1-gcamp3*) (Chen et al., 2012). We performed all ex vivo experiments in 8- to 12-week-old F1 hybrid mice, which do not yet manifest seizures, giving us the opportunity to study how MeCP2 dysfunction disrupts spontaneous circuit activity. We prepared coronal slices containing dorsal hippocampus from F1 males at 8 weeks of age and F1 female *Mecp2*^{+/-} mice at 12 weeks, when these models develop hippocampus-dependent learning abnormalities (Collins et al., 2004; Guy et al., 2001; Samaco et al., 2013), and imaged calcium events in hippocampal CA1 pyramidal neurons by two-photon microscopy (see Experimental Procedures; Figures 1A and 1B; Movie S1, available online). We recorded activity from multiple neurons simultaneously (median 11 per field of view, range 2–22) (Figure 1B). GCaMP3 accurately represented CA1 pyramidal neuron spiking in our preparation (Figure S1A) as reported previously (Chen et al., 2012). Analysis was performed on the averaged fluorescence trace thresholded to detect events and exclude noise (Figure S1B; see Experimental Procedures).

Neurons from *Mecp2* null mice (Null) had lower event rates and event amplitudes than neurons of wild-type (WT) mice, whereas neurons from mice overexpressing *MECP2* (Tg1) showed higher event rates and amplitudes (Figures S1C and S1D). Both mutant genotypes, however, showed synchronization of activity across simultaneously imaged neurons (Figures 1C and 1D). As seen in the example heatmaps of calcium activity (Figure 1C), WT neurons (top) were asynchronous, firing relatively independently in time, while in Null and Tg1 mice there are clear examples of multi-neuron ensembles activating simultaneously (i.e., synchronously). This effect was apparent when comparing the cumulative interneuronal correlation coefficient distributions across all pairs (Figures 1D and S1E) or the mean correlation coefficient as a function of distance between neurons (Figure 1D, insets). The elevated synchrony in mutants was not due to differences in the event rate (Figure S1F). Twelve-week-old *Mecp2*^{+/-} female mice (hereafter referred to as Rett) showed a similar effect (Figures 1C and 1D, purple), demonstrating that mosaic loss of MeCP2, as occurs in Rett syndrome patients, also generates CA1 hypersynchrony. Normal levels of MeCP2 are required for neural circuits to maintain the asynchronous network state.

Next, we confirmed that neuronal hypersynchrony also occurs in *Mecp2* mutant mice in vivo by single-unit recording. Tetrodes were implanted into hippocampal CA1 (Cheng and Ji, 2013) of Rett mice and WT littermates (Figure 1E), and ensembles of single units were recorded as animals stood on a small platform (Figure 1F). Pearson correlation coefficients computed from the firing rates (binned at 167 ms as in calcium imaging data) revealed a significant increase in the synchrony of neurons in Rett mice compared to WT during quiescent wakefulness (Figure 1G). Increased synchrony in Rett mice was observed at a wide range of firing rate bin sizes (5–200 ms; Figure 1G, inset) and was also present during active wakefulness (Figure 1G, inset, dotted lines). Average firing rates were similar between genotypes (WT, 0.57 ± 0.14 Hz; Rett, 0.65 ± 0.12 Hz during quiescent wakefulness). No electrophysiological signatures of epileptic activity in the hippocampus were observed in any WT or Rett mice that were studied. These data show that *Mecp2* mutations produce abnormally increased synchrony between CA1 neurons in vivo, similar to what we observed with hippocampal slices.

We then monitored spontaneous hippocampal activity before and after bath application of the GABA_A receptor antagonist Gabazine (Figures 2A and S2A). Low-dose GABA blockade (0.5–1 μM Gabazine), which blocks approximately 10%–30% of GABA_A receptors (Uchida et al., 1996), increased synchrony more dramatically in neurons from Null (blue), Tg1 (orange), and Rett (purple) mice than neurons from their control littermates (Figures 2A–2C and S2A; Movies S1 and S2), revealing an impaired ability of the *Mecp2* mutants to maintain the asynchronous network state in the presence of Gabazine. This effect was consistent in the presence of Gabazine over a range of different concentrations (0.5, 1, and 10 μM; Figure S2B). Given that the increase in mean interneuronal correlation strength observed in the mutants after Gabazine application is greater than would be expected purely on the basis of differences seen at baseline (pre-Gabazine condition) (Figure 2C), this suggests a failure of homeostasis. Low-dose GABA blockade led to increased synchrony in mutants even after lesioning the CA3 to CA1 Schaffer collateral (SC) input (Figure S2C), suggesting that hypersynchrony is attributable, at least in part, to changes in the local CA1 circuitry. Lesioning the SC input in the absence of GABA blockade also increased synchrony in Tg1 mice (Figure S2D), but not Null mice (data not shown), indicating synchrony-favoring local circuit abnormalities in *MECP2*-overexpressing CA1.

To examine the role that MeCP2 plays in different types of neurons in the development of CA1 hypersynchrony, we employed conditional knockout (cKO) and overexpression (cOE) genetic techniques. We generated cKO mice that lacked MeCP2 either in excitatory pyramidal neurons (*Vglut2-Cre*^{+/-}; *Mecp2*^{fllox+/y}, E-cKO; Figure 2D, teal), in somatostatin-positive (SST) inhibitory neurons (*SST-Cre*^{+/-}; *Mecp2*^{fllox+/y}, SST-cKO; Figure 2D, magenta), or in parvalbumin-positive (PV) inhibitory interneurons (*PV-Cre*^{+/-}; *Mecp2*^{fllox+/y}, PV-cKO; Figure 2D, maroon). We also generated cOE mice that overexpressed MeCP2 specifically in excitatory neurons by breeding *Vglut2-Cre*^{+/-} male mice to females carrying an *Mecp2* conditional rescue allele with a floxed STOP cassette (*Mecp2*^{L^{SL}/+}) (Guy et al., 2007) and *Tg1* allele (*Vglut2-Cre*^{+/-}; *Mecp2*^{L^{SL}/y}; *MECP2*^{Tg1}, E-cOE; Figure 2D, light

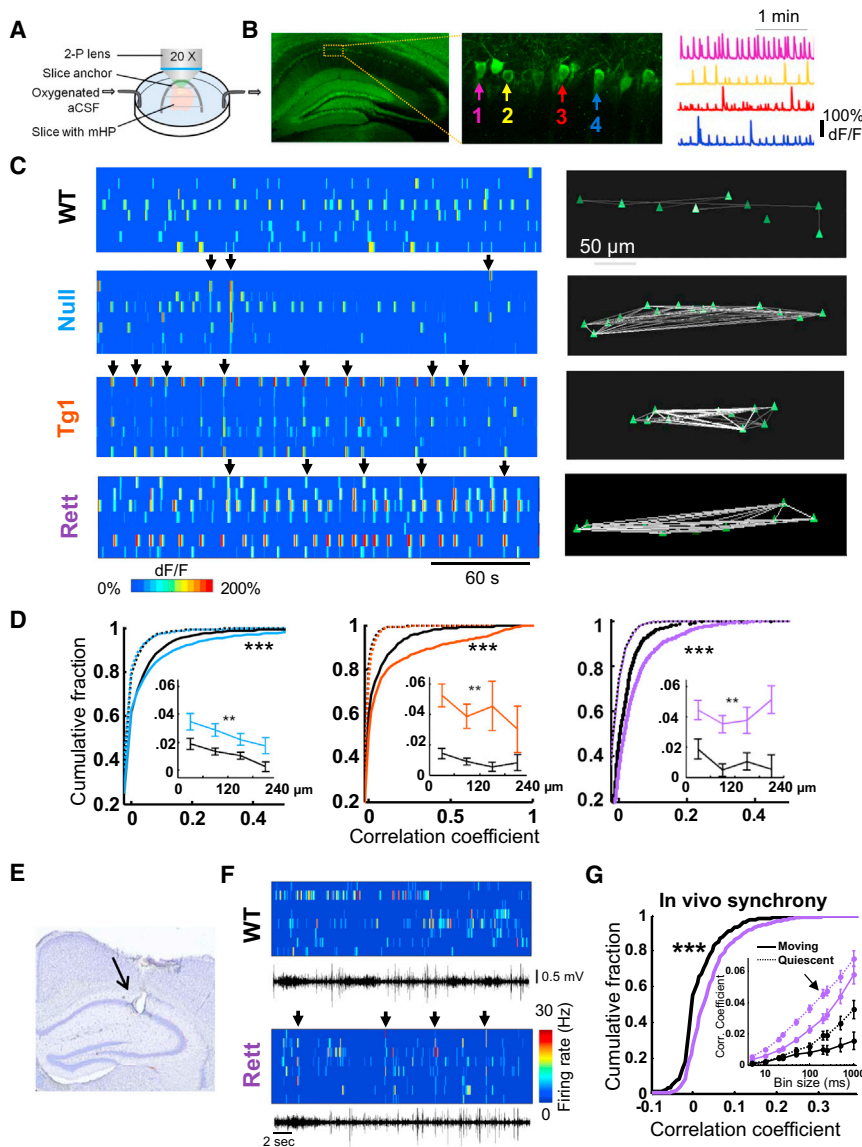


Figure 1. Loss of the Asynchronous Network State in Hippocampal CA1 of MeCP2 Mutant Mice

(A) Schematic of ex vivo two-photon imaging. (B) Left: two-photon image of hippocampal slice from a thy1-GCaMP3 mouse. Box: pyramidal layer of hippocampal CA1. Middle: high-magnification image of GCaMP3-labeled CA1 pyramidal neurons. Right: sample dF/F (percent change in fluorescence intensity; see [Experimental Procedures](#)) calcium traces from four simultaneously imaged neurons labeled with arrows in the middle image.

(C) Left: representative heatmap plots of calcium transients. Each row is a neuron; each column is an imaging frame (~167 ms). Arrows point to synchronous events. Right: graph visualization of all neurons recorded simultaneously in this experiment. The location of each neuron is denoted by a triangle. Each neuron's event rate is represented by the triangle's brightness (linear scale, range 0.003–0.3 Hz). Significant positive correlations between neurons (two SD above the shuffled distribution mean; see [Experimental Procedures](#)) are plotted as graph edges, where the thickness/brightness of the edge signifies the strength of the positive correlation (linear scale, range 0–0.6).

(D) Cumulative histogram of interneuronal correlation coefficients per cell pair in Null (blue, left), Tg1 (orange, middle), and Rett (purple, right) mice versus wild-type (WT) littermates (black). Dotted lines represent shuffled correlation distributions calculated from calcium traces circularly permuted in time (see [Experimental Procedures](#)). *** $p < 0.001$, Mann-Whitney U test or Kolmogorov-Smirnov test. Insets: mean Pearson correlation per cell pair as a function of distance between cells in Null (left) and Tg1 (right). ** $p < 0.01$, ANOVA.

(E) Example bright-field image of coronal hippocampal slice from a tetrode-implanted animal. Arrow indicates electrolytic lesion produced by the tip of the tetrode, confirming localization in stratum pyramidale of CA1.

(F) Heatmap depiction of simultaneously recorded tetrode single-unit firing rates in hippocampal CA1 of Rett mice (bottom) and WT littermates (top) during quiescent wakefulness. Arrows point to

synchronous events. Black traces show the simultaneously recorded hippocampal local field potential, high-pass filtered to show ripple events.

(G) Cumulative histogram of correlation coefficients measured from Rett mice (purple, $n = 739$ pairs, 123 neurons, 6 animals) and WT mice (black, $n = 569$ pairs, 100 neurons, 5 animals). *** $p < 0.0001$, Mann-Whitney U test or Kolmogorov-Smirnov test. Inset, correlation coefficient at each time bin size for Rett and WT mice, in the awake quiescent (dotted line) and awake moving (solid line) state. Note that pairwise neuronal correlations are consistently elevated in Rett mice across firing rate bin sizes in both behavioral states. Arrow points to the bin size (167 ms) of the datasets used in (F) and the cumulative histogram. Error bars represent mean \pm SE.

orange). Calcium activity in hippocampal CA1 neurons was acquired before and after low-dose GABA blockade in cKO/cOE mice and littermate controls ([Figure 2D](#)). Remarkably, elevated baseline (pre-drug) synchrony was observed in CA1 pyramidal neurons recorded from mice that selectively lacked (E-cKO) or overexpressed (E-cOE) MeCP2 in excitatory cells, but not from neurons in mice that selectively lacked MeCP2 in inhibitory neurons (SST-cKO and PV-cKO). In contrast, low-dose GABA blockade drove profound hypersynchrony in the SST-cKO and PV-cKO, but a much smaller increase in synchrony in the E-cKO compared to constitutive *Mecp2* KO (compare [Figure 2D](#)

to [Figure 2C](#)), and no increase in the E-cOE relative to control. These data suggest that MeCP2 in inhibitory interneurons plays a key role in maintaining the asynchronous state in response to perturbations that tip the balance of excitation versus inhibition.

A recent modeling study of hippocampal dysfunction in Rett syndrome specifically predicted a loss of excitatory synaptic response in inhibitory neurons ([Ho et al., 2014](#)). We therefore tested this possibility in hippocampal CA1 oriens-layer interneurons, the majority of which receive excitatory glutamatergic input from the axon collaterals of CA1 pyramidal neurons and mediate feedback dendritic inhibition to these pyramidal neurons ([Müller](#)

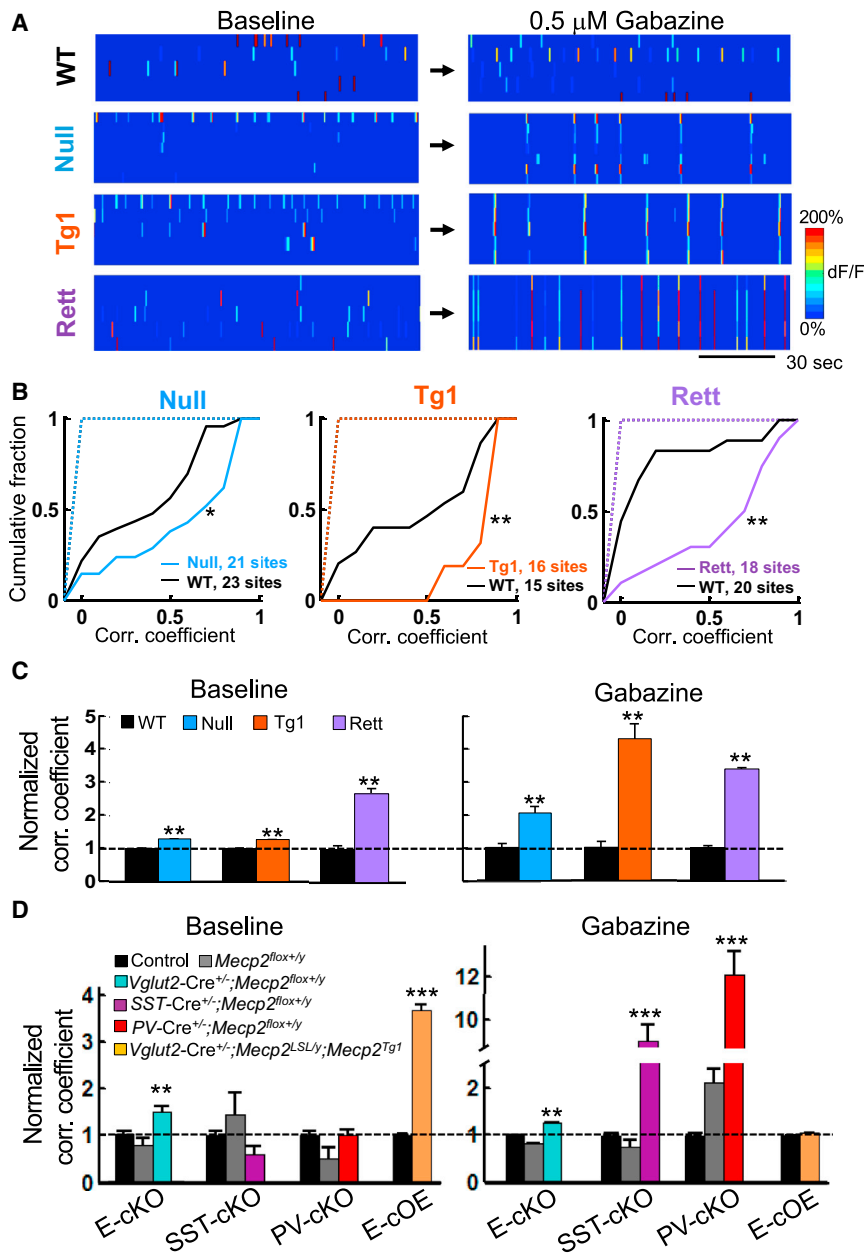


Figure 2. Loss of Neural Circuit Homeostasis in Models of MeCP2 Disorders

(A) Heatmap depiction of example traces from WT, Null, Tg1, and female heterozygous Rett CA1 pyramidal neurons before (left) and after (right) bath application of small amounts (0.5 μ M) of the GABA_A receptor blocker Gabazine.

(B) Cumulative histogram of inter-neuronal correlation coefficients per imaging site obtained with low-dose Gabazine in Null (blue, left), Tg1 (orange, middle), and Rett (purple, right) mice versus WT littermates (black). Dotted lines represent shuffled correlation distributions (see [Experimental Procedures](#)). *p < 0.05, **p < 0.01, Mann-Whitney U test or Kolmogorov-Smirnov test.

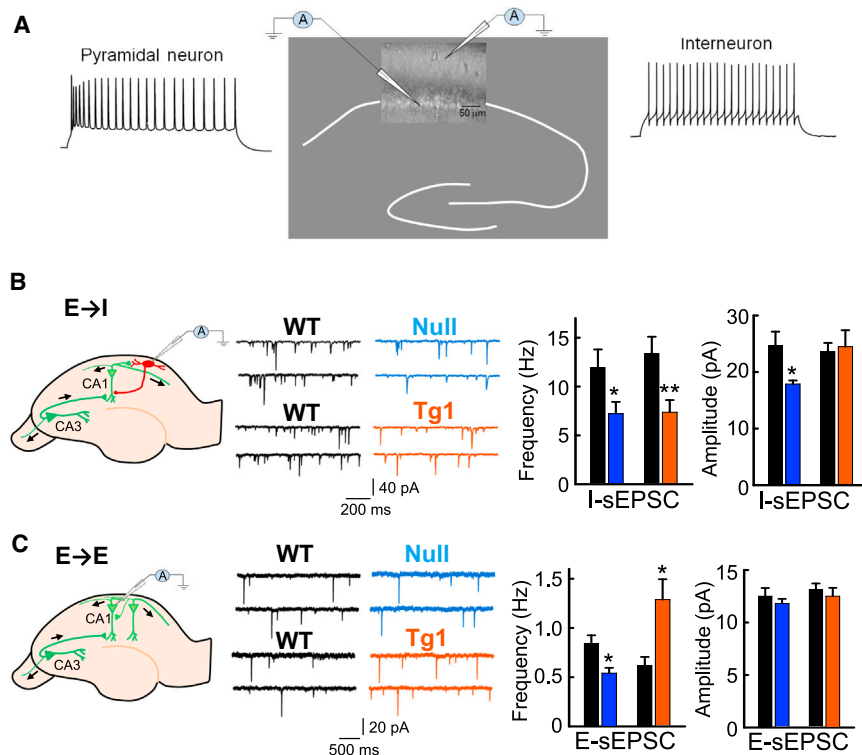
(C) Normalized mean CA1 pyramidal neuron correlation (corr.) coefficients of Null, Tg1, Rett mice, and WT littermates at baseline and with low-dose Gabazine. Correlation coefficient of the mutants was normalized to WT at baseline and with low-dose Gabazine, respectively. Note that correlation coefficient strength in the mutants was disproportionately increased after low-dose Gabazine compared to baseline. **p < 0.01, ***p < 0.0001, Mann-Whitney U test, analyzed per pair. See [Table S1](#) for n numbers.

(D) Normalized mean correlation (corr.) coefficients of CA1 pyramidal neuron in excitatory-specific *Mecp2* knockout mice (E-cKO, teal), somatostatin neuron-specific KO (SST-cKO, magenta), parvalbumin neuron-specific KO (PV-cKO, maroon), and excitatory-specific *Mecp2* overexpression (E-cOE, light orange) mice and control littermates at baseline and with low-dose Gabazine. Correlation coefficient of the mutants was normalized to control (combination of WT and Cre) at baseline and with low-dose Gabazine, respectively. **p < 0.01, ***p < 0.0001, Mann-Whitney U test, analyzed per pair. See [Table S1](#) for n numbers. Error bars represent mean \pm SE.

and Remy, 2014) (Figures 3A and 3B). Remarkably, the frequency of spontaneous excitatory postsynaptic currents (sEPSCs) in oriens-layer interneurons was decreased by about 40% in both Null and Tg1 mice (Figure 3B), revealing a profound impairment in excitatory synaptic response in the inhibitory neurons of the hippocampal circuit. The amplitude of sEPSCs was also decreased by 30% in Null interneurons. The impairment on sEPSC frequency in inhibitory neurons occurred in both excitatory neuron-specific cKO mice (E-cKO) and SST+ inhibitory neuron-specific cKO mice (SST-cKO) (Figure S3A). This shows that normal MeCP2 function is required in both the presynaptic and postsynaptic neurons to maintain normal excitatory-to-inhibitory synaptic function. As previously reported (Chao

et al., 2007), connectivity between excitatory neurons was increased in Tg1 mice and decreased in Null mice (Figure 3C). The basic function of inhibitory synapses onto excitatory CA1 neurons was normal in both Null and Tg1 mice (Figures S3B and S3C). Thus, decreased

excitatory synaptic responses in oriens-layer interneurons, which could lead to reduced recurrent inhibition during spontaneous activity, are a shared synaptic abnormality in MeCP2 disorders. Finally, we explored the effects of DBS of the fornix on these phenotypes, since DBS normalizes hippocampus-dependent learning and memory in Rett mice (Hao et al., 2015). We therefore implanted 6- to 8-week-old Rett mice and WT littermates with chronic stimulating electrodes targeted unilaterally to the fimbria-fornix under the guidance of evoked potential recordings in the hippocampus (Figure 4A). Mice in the DBS group received daily DBS for 2 weeks (Hao et al., 2015), and mice in the sham group underwent identical procedures except for DBS. We



performed experiments 3 weeks after the last stimulation session, matched to the time of behavioral rescue (Hao et al., 2015). Chronic DBS, but not sham DBS, normalized synchrony between CA1 pyramidal neurons to WT-like levels (Figure 4B) and restored the mutant circuit's homeostatic responsiveness (Figures 4C and 4D). Interestingly, DBS did not affect baseline CA1 synchrony in WT animals, but had the opposite effect on their homeostatic response, exacerbating Gabazine-mediated elevation of correlations in WT (Figure 4C). Event rate and event amplitude of Ca^{2+} traces were the same in Rett and WT mice, and were unaffected by DBS (Figure S4A).

We next measured the effect of DBS on the impaired excitatory synaptic response in oriens-layer interneurons. Because *Mecp2* is an X-linked gene and has mosaic expression in Rett syndrome mice and humans (Chahrouh and Zoghbi, 2007), we were able to record from both MeCP2-lacking and MeCP2-expressing neurons in the same animal (Figure 4E). In total, 40%–50% of oriens-layer interneurons also express the neuropeptide SST (Figure 4E). Similar to our previous observations in Null and Tg1 mice (Figure 3B), the frequency of sEPSCs was decreased by about 50% in MeCP2-lacking interneurons compared to MeCP2-expressing interneurons in sham-treated Rett mice (Figure 4G, left), revealing a profound impairment in excitatory synaptic response in MeCP2-lacking inhibitory cells. It was also significantly lower than that measured in sham- or DBS-treated WT mice. Spontaneous EPSC amplitude was also decreased in interneurons lacking MeCP2 (Figure 4G, right). Remarkably, DBS restored sEPSC frequency and amplitude in MeCP2-lacking interneurons back to WT-like (or slightly higher) levels (Figure 4G). The effect of MeCP2 loss and the normalizing effect of

DBS were the same for both SST-positive and SST-negative neurons (Figure S4B), suggesting that these phenotypes occur across multiple subtypes of inhibitory neurons in stratum oriens. Notably, the effect of MeCP2 loss, as well as that of DBS-mediated rescue on excitatory synaptic function in interneurons, is specific to cells lacking MeCP2. This rules out a range of potential confounds that could arise due to differences in slice composition and, furthermore, indicates that DBS intervention is exceptionally specific.

DISCUSSION

We found that hippocampal CA1 hypersynchrony is a feature of both Rett and *MECP2* duplication syndrome models. Conditional loss- and gain-of-function studies show that excitatory neurons depend on normal MeCP2 function to maintain the asynchronous state at baseline, whereas inhibitory interneurons require MeCP2 to enable the circuit to resist hypersynchrony in the face of perturbations to the excitation/inhibition balance. We also found weakened excitatory synaptic response in oriens-layer interneurons, a shared synaptic dysfunction in all three models, and that DBS rescued these phenotypes of hippocampal circuit dysfunction in Rett mice.

Studies of human patients using electroencephalography or fMRI technology reveal that increased neural circuit synchrony might be a hallmark of neuropsychiatric disease, including epilepsy, schizophrenia, and movement disorders such as Parkinson disease, Huntington disease, tremor, and dystonia (Uhlhaas and Singer, 2006). Here we find elevated synchrony in the spontaneous firing activity of hippocampal CA1 neurons, in both MeCP2 deletion and duplication mouse models, ex vivo and in vivo (Figure 1). Of note, this increased synchrony occurs months before the animals develop any seizures, pinpointing

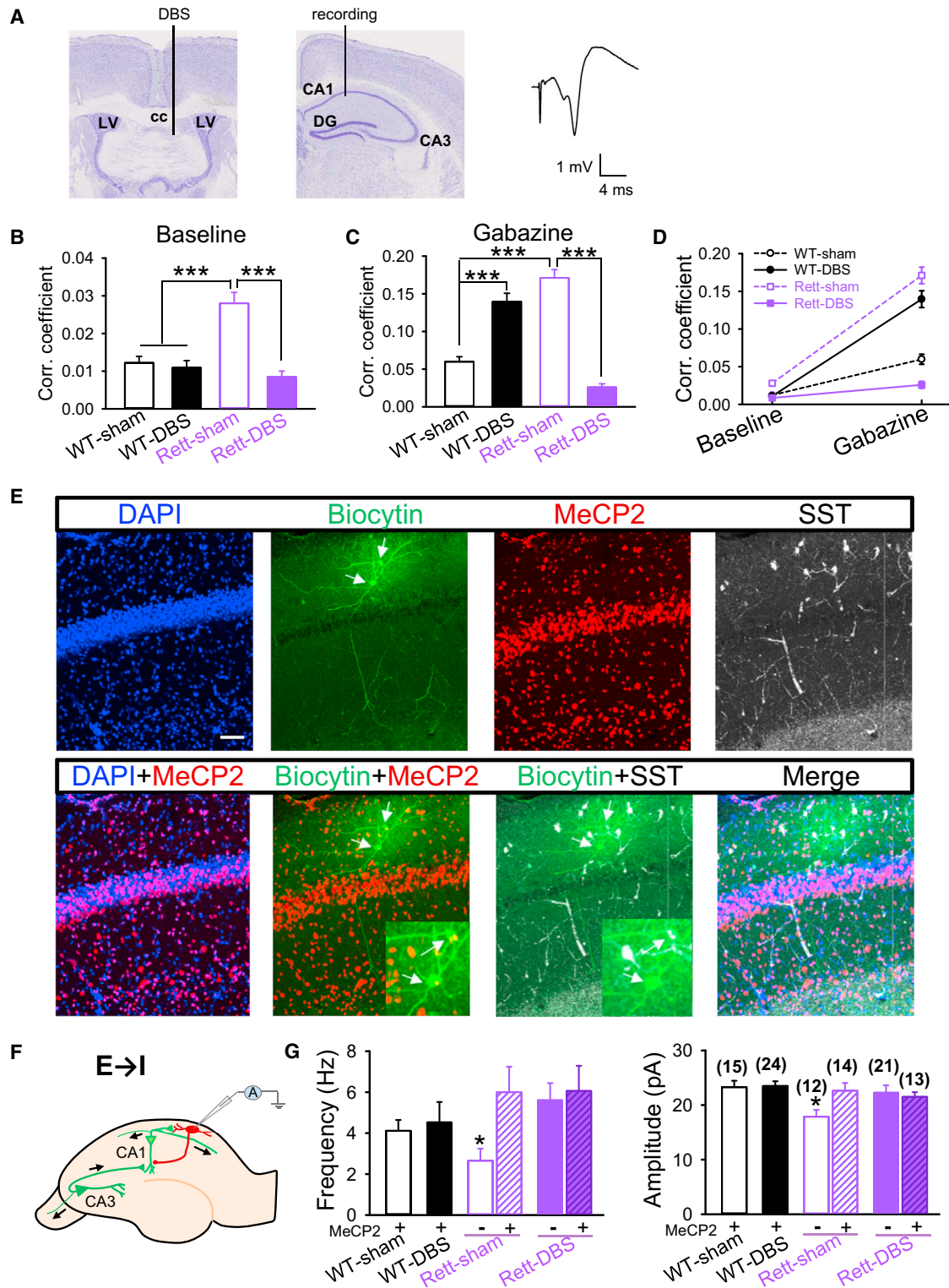


Figure 4. Forniceal DBS Rescued the Abnormal Network Activity and Synaptic Transmission in Hippocampus of Rett Mice

(A) Bright-field picture of coronal sections illustrating the placement of the DBS electrode in the fornix (left) and the recording electrode in CA1 (middle). cc, corpus callosum; LV, lateral ventricle; DG, dentate gyrus. Right: representative evoked potential trace of the fimbria-fornix pathway recorded in CA1.

(legend continued on next page)

early circuit abnormalities. These data suggest that loss of hippocampal circuit asynchrony may contribute to learning and memory abnormalities seen in pediatric neurological syndromes, potentially by degrading the precision of neuronal ensemble firing and disrupting normal circuit dynamics underlying memory formation. The fact that two mouse models with opposite molecular and cellular phenotypes produce the same circuit-level phenotype raises the possibility that our findings may be generalizable to other forms of syndromic intellectual disabilities. Indeed, hypersynchrony in the developing neocortex and increased correlations in the prefrontal cortex were also observed in two other mouse models of autism (Gonçalves et al., 2013; Luongo et al., 2016).

Homeostatic mechanisms governing the balance of excitation and inhibition are in place to prevent runaway excitation, i.e., to maintain circuit asynchrony (Okun and Lampl, 2008). We found that hippocampal CA1 neurons in both MeCP2 deletion and duplication mice are prone to entering a hypersynchronous state in response to a low dose of GABA_A receptor blocker Gabazine (Figure 2) (Bodda et al., 2013; McLeod et al., 2013). This shows that the homeostatic mechanisms maintaining CA1 circuit asynchrony are impaired in both MeCP2 deletion and duplication mice. MeCP2 heterozygous females, the model for Rett syndrome, also showed this dramatic impairment in maintenance of asynchrony. The impaired homeostatic response to perturbations also probably underlies the seizures in late-stage MECP2 duplication patients and mice (Bodda et al., 2013; Collins et al., 2004), and many Rett patients and certain Rett mouse models (Chao et al., 2010; Goffin et al., 2014; Nissenkorn et al., 2010; Zhang et al., 2014). These results provide further evidence for overlapping circuit-level dysfunction phenotypes in these two distinct MeCP2 disorders.

By manipulating MeCP2 dosage in different neuronal subtypes, we found that baseline neuronal synchronization and perturbation-induced hypersynchrony (Figure 2C) are in fact dissociable processes and appear to arise from MeCP2 dysfunction in different groups of neurons (Figure 2D). Normal MeCP2 dosage in excitatory, but not inhibitory, neurons was required to generate the baseline asynchronous state, while MeCP2 in inhibitory, but not excitatory, neurons was needed to maintain circuit asynchrony in response to perturbations. Given that the baseline asynchronous state enables optimal information processing, and maintaining asynchrony in response to perturbations is important to prevent epileptogenesis (Goffin et al., 2014), it is interesting to speculate that different phenotypes

of complex pediatric neurological disorders, e.g., cognitive dysfunction and seizures, may depend on loss of a gene's function in different cell types (Durand et al., 2012). Our results show that different cell types in the hippocampal circuit can play unique roles in the regulation of neural circuit homeostasis.

Decreased excitatory synaptic response in inhibitory interneurons is a shared physiological abnormality between KO and OE mutants that has not been previously reported. We observed an ~40% decrease in the frequency of excitatory synaptic response in these interneurons, suggestive of a dramatic decrease in the number or release probability of excitatory synapses on these cells, which likely disrupts their ability to regulate the timing and plasticity of pyramidal neuron activity (Müller and Remy, 2014). This shared deficit in excitatory synaptic response is unique to interneurons, as excitatory-to-excitatory neuron events (sEPSCs) are decreased in Null but increased in Tg1 mice. Remarkably, the impaired excitatory response in interneurons was also present in both excitatory-specific and inhibitory-specific cKO mice. This showed that there is not a simple one-to-one correspondence between the synaptic physiology and population-level synchrony findings, suggesting that MeCP2 regulates synaptic function in both the presynaptic and postsynaptic cells. Together with the synchrony results, these data suggest that impaired excitatory input to inhibitory neurons could contribute to both baseline and Gabazine-induced hypersynchrony. How this synaptic defect contributes to circuit hypersynchrony needs further exploration.

The shared circuit-level phenotype we report here in both *Mecp2*-deletion and *MECP2*-duplication mice is remarkable given that gain and loss of MeCP2 function largely exert opposing effects on gene expression, synaptic function, and neuronal morphology. This finding opens the exciting possibility that shared circuit-level phenotypes might occur across other mirror-image deletion-duplication genomic disorders such as Smith-Magenis syndrome (chr17p deletion) and Potocki-Lupski syndrome (chr17p duplication) (Ramocki and Zoghbi, 2008) or the 16p11.2 deletion and duplication syndromes (Qureshi et al., 2014). Future studies investigating this possibility might inspire targeted circuit manipulations that could potentially benefit a broad class of disorders characterized by syndromic cognitive dysfunction.

DBS might provide just such a circuit manipulation. DBS is already commonly employed for Parkinson disease and dystonia. Its use is being explored in a wide range of neuropsychiatric disease including epilepsy, Alzheimer, Tourette syndrome, and

(B and C) Summary of averaged interneuronal correlation coefficients per imaging site obtained before (B) and after (C) bath application of 0.5 μ M Gabazine in DBS- or sham-treated Rett mice (purple) versus WT littermates (black). *** $p < 0.001$, ANOVA.

(D) Comparison of averaged interneuronal correlation coefficients per imaging site obtained before and after bath application of 0.5 μ M Gabazine in DBS- or sham-treated Rett mice (purple) versus WT littermates (black). Refer to (B) and (C) for statistics; same dataset is used.

(E) Sample images showing immunostaining for DAPI, biocytin, MeCP2, and somatostatin (SST) in a slice from Rett mice with two oriens-layer interneurons recorded for sEPSCs via class pipettes loaded with 0.2% biocytin. White arrows indicate the soma of interneurons recorded. Both interneurons are MeCP2 positive and only one of them is SST positive. The merged image of DAPI and MeCP2 staining showed mosaic expression of MeCP2. Scale bar, 50 μ m. Insert: zoom-in image of soma area.

(F) Experiment schematic of recordings from oriens-layer interneuron.

(G) Mean sEPSC frequency (left) and amplitude (right) of sEPSC measured from CA1 oriens-layer interneurons in DBS- or sham-treated Rett mice (purple) versus WT littermates (black). Numbers in parentheses represent the number of neurons recorded for each condition. Frequency (left) and amplitude (right) of sEPSC were calculated from the same set of neurons. * $p < 0.05$ to all other groups, t test.

Error bars represent mean \pm SE.

depression, yet the biological mechanisms underlying the resolution of symptoms following DBS are hardly studied and poorly understood. This is especially true for chronic DBS paradigms, which must mediate their effect through enduring changes in circuit connections and function. Here we show that chronic DBS can modify synaptic microcircuits in a manner that both repairs neural circuit homeostasis and normalizes spatiotemporal patterns of spontaneous firing activity in a heritable form of intellectual disability. Our finding that DBS rescues both the learning deficit (Hao et al., 2015) and circuit dysfunction suggests that these circuit abnormalities may underlie, or at least contribute to, the behavioral deficits in Rett mice. This supports the notion that Rett and related syndromes are disorders of neural circuit function, or “circuitopathies,” and therefore may respond to interventions targeted at the neural circuit level (Zoghbi and Bear, 2012). Finally, DBS shows promise for restoring neurological dysfunction in carefully selected disorders of autism and intellectual disability, where there are perhaps hundreds of distinct genetic etiologies that converge to a few regimes of canonical neural circuit dysfunction.

EXPERIMENTAL PROCEDURES

All procedures to maintain and use these mice were approved by the Institutional Animal Care and Use Committee for Baylor College of Medicine and Affiliates. A full description of Experimental Procedures is found in the [Supplemental Experimental Procedures](#).

SUPPLEMENTAL INFORMATION

Supplemental Information includes Supplemental Experimental Procedures, four figures, one table, and two movies and can be found with this article online at <http://dx.doi.org/10.1016/j.neuron.2016.07.018>.

AUTHOR CONTRIBUTIONS

H.L., R.T.A., S.M.S., and H.Y.Z. designed the experiments and reviewed and interpreted data. H.L., S.E.K., L.H., W.W., and D.Y. performed the experiments. S.H. and B.T. implanted the DBS electrode. R.T.A. and S.E.K. performed the data analysis in MATLAB. K.U., X.M., and A.I.-I. provided the female cKO mice for breeding. Y.S. genotyped the mice. H.L. and R.T.A. wrote the manuscript with critical input from D.J., J.T., B.R.A., S.M.S., and H.Y.Z.

ACKNOWLEDGMENTS

We thank Guoping Feng for providing the thy1-GCaMP3 mouse line. This work was supported by funding from NIH 5R01NS057819 to H.Y.Z. and NIH 1K99NS089824 to H.L., grants from the Simons Foundation and March of Dimes to S.M.S., the W.M. Keck Foundation (H.Y.Z.), the Autism Speaks Weatherstone Fellowship, Medical Scientist Training Program to R.T.A., the Cockrell Family Foundation, the Rett Syndrome Research Trust, Carl C. Anderson, Sr. and Marie Jo Anderson Charitable Foundation, and the Howard Hughes Medical Institute (H.Y.Z.). The work was also supported in part by the Behavioral Core, the Neuroconnectivity Core, and the Microscopy Core of IDDRC at Baylor College of Medicine and supported by NIH 1 U54 HD083092 from the Eunice Kennedy Shriver National Institute of Child Health and Human Development.

Received: March 8, 2015
 Revised: May 1, 2016
 Accepted: July 7, 2016
 Published: August 4, 2016

REFERENCES

- Bodda, C., Tantra, M., Mollajew, R., Arunachalam, J.P., Laccone, F.A., Can, K., Rosenberger, A., Mironov, S.L., Ehrenreich, H., and Mannan, A.U. (2013). Mild overexpression of *MeCP2* in mice causes a higher susceptibility toward seizures. *Am. J. Pathol.* *183*, 195–210.
- Chahrouh, M., and Zoghbi, H.Y. (2007). The story of Rett syndrome: from clinic to neurobiology. *Neuron* *56*, 422–437.
- Chahrouh, M., Jung, S.Y., Shaw, C., Zhou, X., Wong, S.T.C., Qin, J., and Zoghbi, H.Y. (2008). MeCP2, a key contributor to neurological disease, activates and represses transcription. *Science* *320*, 1224–1229.
- Chao, H.-T., Zoghbi, H.Y., and Rosenmund, C. (2007). MeCP2 controls excitatory synaptic strength by regulating glutamatergic synapse number. *Neuron* *56*, 58–65.
- Chao, H.-T., Chen, H., Samaco, R.C., Xue, M., Chahrouh, M., Yoo, J., Neul, J.L., Gong, S., Lu, H.-C., Heintz, N., et al. (2010). Dysfunction in GABA signaling mediates autism-like stereotypies and Rett syndrome phenotypes. *Nature* *468*, 263–269.
- Chen, Q., Cichon, J., Wang, W., Qiu, L., Lee, S.J., Campbell, N.R., Destefino, N., Goard, M.J., Fu, Z., Yasuda, R., et al. (2012). Imaging neural activity using Thy1-GCaMP transgenic mice. *Neuron* *76*, 297–308.
- Cheng, J., and Ji, D. (2013). Rigid firing sequences undermine spatial memory codes in a neurodegenerative mouse model. *eLife* *2*, e00647.
- Collins, A.L., Levenson, J.M., Vilaythong, A.P., Richman, R., Armstrong, D.L., Noebels, J.L., David Sweatt, J., and Zoghbi, H.Y. (2004). Mild overexpression of MeCP2 causes a progressive neurological disorder in mice. *Hum. Mol. Genet.* *13*, 2679–2689.
- Durand, S., Patrizi, A., Quast, K.B., Hachigian, L., Pavlyuk, R., Saxena, A., Carninci, P., Hensch, T.K., and Fagioli, M. (2012). NMDA receptor regulation prevents regression of visual cortical function in the absence of *MeCP2*. *Neuron* *76*, 1078–1090.
- Goffin, D., Brodtkin, E.S., Blendy, J.A., Siegel, S.J., and Zhou, Z. (2014). Cellular origins of auditory event-related potential deficits in Rett syndrome. *Nat. Neurosci.* *17*, 804–806.
- Gonçalves, J.T., Anstey, J.E., Golshani, P., and Portera-Cailliau, C. (2013). Circuit level defects in the developing neocortex of Fragile X mice. *Nat. Neurosci.* *16*, 903–909.
- Guy, J., Hendrich, B., Holmes, M., Martin, J.E., and Bird, A. (2001). A mouse *MeCP2*-null mutation causes neurological symptoms that mimic Rett syndrome. *Nat. Genet.* *27*, 322–326.
- Guy, J., Gan, J., Selfridge, J., Cobb, S., and Bird, A. (2007). Reversal of neurological defects in a mouse model of Rett syndrome. *Science* *315*, 1143–1147.
- Hao, S., Tang, B., Wu, Z., Ure, K., Sun, Y., Tao, H., Gao, Y., Patel, A.J., Curry, D.J., Samaco, R.C., et al. (2015). Forniceal deep brain stimulation rescues hippocampal memory in Rett syndrome mice. *Nature* *526*, 430–434.
- Ho, E.C.Y., Eubanks, J.H., Zhang, L., and Skinner, F.K. (2014). Network models predict that reduced excitatory fluctuations can give rise to hippocampal network hyper-excitability in MeCP2-null mice. *PLoS ONE* *9*, e91148.
- Huxter, J., Burgess, N., and O’Keefe, J. (2003). Independent rate and temporal coding in hippocampal pyramidal cells. *Nature* *425*, 828–832.
- Jiang, M., Ash, R.T., Baker, S.A., Suter, B., Ferguson, A., Park, J., Rudy, J., Torsky, S.P., Chao, H.T., Zoghbi, H.Y., and Smirnakis, S.M. (2013). Dendritic arborization and spine dynamics are abnormal in the mouse model of MECP2 duplication syndrome. *J. Neurosci.* *33*, 19518–19533.
- Luongo, F.J., Horn, M.E., and Sohal, V.S. (2016). Putative microcircuit-level substrates for attention are disrupted in mouse models of autism. *Biol. Psychiatry* *79*, 667–675.
- McLeod, F., Ganley, R., Williams, L., Selfridge, J., Bird, A., and Cobb, S.R. (2013). Reduced seizure threshold and altered network oscillatory properties in a mouse model of Rett syndrome. *Neuroscience* *237*, 195–205.

- Mehta, M.R. (2015). From synaptic plasticity to spatial maps and sequence learning. *Hippocampus* 25, 756–762.
- Müller, C., and Remy, S. (2014). Dendritic inhibition mediated by O-LM and bistripartite interneurons in the hippocampus. *Front. Synaptic Neurosci.* 6, 23.
- Nissenkorn, A., Gak, E., Vecsler, M., Reznik, H., Menascu, S., and Ben Zeev, B. (2010). Epilepsy in Rett syndrome—the experience of a National Rett Center. *Epilepsia* 51, 1252–1258.
- Okun, M., and Lampl, I. (2008). Instantaneous correlation of excitation and inhibition during ongoing and sensory-evoked activities. *Nat. Neurosci.* 11, 535–537.
- Qureshi, A.Y., Mueller, S., Snyder, A.Z., Mukherjee, P., Berman, J.I., Roberts, T.P., Nagarajan, S.S., Spiro, J.E., Chung, W.K., Sherr, E.H., and Buckner, R.L.; Simons VIP Consortium (2014). Opposing brain differences in 16p11.2 deletion and duplication carriers. *J. Neurosci.* 34, 11199–11211.
- Ramocki, M.B., and Zoghbi, H.Y. (2008). Failure of neuronal homeostasis results in common neuropsychiatric phenotypes. *Nature* 455, 912–918.
- Ramocki, M.B., Tavyev, Y.J., and Peters, S.U. (2010). The MECP2 duplication syndrome. *Am. J. Med. Genet. A.* 152A, 1079–1088.
- Renart, A., de la Rocha, J., Bartho, P., Hollender, L., Parga, N., Reyes, A., and Harris, K.D. (2010). The asynchronous state in cortical circuits. *Science* 327, 587–590.
- Samaco, R.C., McGraw, C.M., Ward, C.S., Sun, Y., Neul, J.L., and Zoghbi, H.Y. (2013). Female *Mecp2*(+/-) mice display robust behavioral deficits on two different genetic backgrounds providing a framework for pre-clinical studies. *Hum. Mol. Genet.* 22, 96–109.
- Uchida, I., Cestari, I.N., and Yang, J. (1996). The differential antagonism by bicuculline and SR95531 of pentobarbitone-induced currents in cultured hippocampal neurons. *Eur. J. Pharmacol.* 307, 89–96.
- Uhlhaas, P.J., and Singer, W. (2006). Neural synchrony in brain disorders: relevance for cognitive dysfunctions and pathophysiology. *Neuron* 52, 155–168.
- Zhang, W., Peterson, M., Beyer, B., Frankel, W.N., and Zhang, Z.W. (2014). Loss of MeCP2 from forebrain excitatory neurons leads to cortical hyperexcitation and seizures. *J. Neurosci.* 34, 2754–2763.
- Zoghbi, H.Y., and Bear, M.F. (2012). Synaptic dysfunction in neurodevelopmental disorders associated with autism and intellectual disabilities. *Cold Spring Harb. Perspect. Biol.* 4, a009886, <http://dx.doi.org/10.1101/cshperspect.a009886>.